Pion-induced pion production on the deuteron

J. Lichtenstadt, D. Ashery, and S. A. Wood*
School of Physics and Astronomy,
The Raymond and Beverly Sackler Faculty of Exact Sciences,
Tel Aviv University, Tel Aviv, Israel

E. Piasetzky,† P. A. M. Gram, and D. W. MacArthur
Los Alamos National Laboratory, Los Alamos, New Mexico 87545

R. S. Bhalerao and L. C. Liu
Isotope and Nuclear Chemistry Division, Los Alamos National Laboratory, Los Alamos, New Mexico 87545

G. A. Rebka, Jr. and D. Roberts
University of Wyoming, Laramie, Wyoming 82071
(Received 11 April 1985)

Pion-induced pion production on the deuteron was studied via the reactions $\pi^+ d \rightarrow \pi^- \pi^+ pp$ and $\pi^- d \rightarrow \pi^+ \pi^- nn$. The doubly differential cross sections for these reactions were measured, covering the center-of-mass phase space at incident pion energies of 256, 331, and 450 MeV. Calculations of the quasifree production process on one nucleon were performed in a plane-wave approximation using a phenomenological, on-shell $\pi^- p \rightarrow \pi^+ \pi^- n$ amplitude. Comparison of the data with the calculations indicates that the quasifree mechanism dominates these production reactions on the deuteron. Upper limits for bound $\pi^- nn$ and $\pi^+ pp$ systems with small binding energies were also measured. The possible existence of a resonance in these systems near the production threshold was investigated.

I. INTRODUCTION

Pion production by pions on nuclei is almost completely unexplored. The dominance of single-pion production in πN inelastic reactions[1] for pion energies up to about 1 GeV suggests that the investigation of $(\pi,2\pi)$ reactions is a natural first step in the study of the reaction mechanisms that occur in nuclei at energies above the (3,3) resonance. In a nucleus the simplest mechanism that contributes to pion production is the quasifree process on a single nucleon. Even in this role the presence of the other nucleons modifies the free $\pi N \rightarrow \pi\pi N$ amplitude. First, it allows the collision to occur off shell; second, it acts as a medium that alters the formation and propagation of intermediate states; and last, it distorts the incoming and outgoing pion waves. Other mechanisms are those in which pairs of nucleons are actively involved in the production of a pion in contrast to processes in which the spectator nucleons mainly contribute to distortions. One such two-nucleon mechanism for $(\pi,2\pi)$ was proposed by Brown *et al.*,[2] who predicted, using the SU(4) quark model, the existence of a strong $\Delta N \rightarrow \Delta\Delta$ transition in systems of two or more nucleons. Subsequent decay of the two Δ's contributes to the $(\pi,2\pi)$ reaction.

The deuteron is the simplest nucleus in which rescattering and two-nucleon mechanisms, even if weak, can exist. However, since it is a loosely bound system, one may expect that the free $\pi N \rightarrow \pi\pi N$ amplitude will be only little affected by the second nucleon. Moreover, the deuteron wave function is well determined up to very high momentum from electron- and proton-scattering experiments. Thus the ingredients for reliable calculations of the quasifree process are available, and a comparison between the $\pi^- d \rightarrow \pi^+ \pi^- nn$ and $\pi^+ d \rightarrow \pi^- \pi^+ pp$ data and the quasifree prediction would yield information about two-nucleon production mechanisms.

With the advantages of studying the $(\pi,2\pi)$ reaction on the deuteron the limitations for observing the two-nucleon mechanism $\Delta N \rightarrow \Delta\Delta$ should still be mentioned. This production channel will not be favored in the deuteron since the intermediate ΔN state will be of $T=1$ whereas the $\Delta\Delta$ state is preferred (by a factor of 3 in the amplitude) with isospin $T=2$. Moreover, being a loosely bound system the creation of a ΔN state will be even further suppressed. So while production on the deuteron is not expected to exhibit strong contributions due to $\Delta\Delta$ intermediate states, it will still provide useful data from which deviations from quasifree processes will be detectable.

Of special interest is the study of the $\pi^- nn$ and $\pi^+ pp$ components in the final state, which are of isospin $T=2$. If the NN system is formed, it has low relative momentum and is likely to be in a $^1S_0$ state with $T=1$. The pion may then be attracted to it through the P_{33} interaction to form a state that may be considered an off-shell ΔN. Moreover, a $T=2$ ΔN state cannot decay by either the strong or the electromagnetic interaction, and thus may appear in the reactions studied here as a narrow resonance or even as a bound state. This subject was recently discussed by Garcilazo,[3] who showed that with certain parametrizations of the πN and NN interactions, the calculations predict the existence of a bound state. However, the uncertainties in our knowledge of these parametriza-

tions and, in particular, of the πN effective range, leave ample room to doubt its existence. In heavier nuclei these $T=2$ ΔN states have additional importance, since they are doorways to the formation of $T=2$ $\Delta\Delta$ states.

We report an experimental study of the $\pi^-d\rightarrow\pi^+\pi^-nn$ and $\pi^+d\rightarrow\pi^-\pi^+pp$ reactions performed at the Clinton P. Anderson Meson Physics Facility (LAMPF). The doubly differential cross sections $d^2\sigma/d\Omega\, dT$ for the production of pions with charges opposite to that of the incident beam were measured at incident kinetic energies of 256, 331, and 450 MeV. The experimental procedure is described in Sec. II. We present the results in Sec. III, where they are also compared with a calculation based on the quasifree pion-production process. The calculation in plane-wave approximation uses the elementary $\pi^-p\rightarrow\pi^+\pi^-n$ experimental amplitudes. It is described in detail along with the parametrization of the free amplitude in Sec. IV. Measured upper limits for production of π^-nn and π^+pp bound systems are given in Sec. V, where we also discuss the possibility of observing a resonance in these systems. First results of this work were published earlier.[4]

II. EXPERIMENTAL PROCEDURE

The measurements of the $\pi^-d\rightarrow\pi^+\pi^-nn$ and $\pi^+d\rightarrow\pi^-\pi^+pp$ reactions were performed at the high-energy pion channel (p^3W) at LAMPF. Since double-charge exchange is impossible on the deuteron, the detection of a pion with a charge opposite to that of the incident one is an unambiguous identification of a pion production. The doubly differential cross sections $d^2\sigma/d\bar{\Omega}\, d\bar{T}$ for the produced pions in both reactions were measured at 35–40 locations uniformly distributed in $\bar{T}$-cos$\bar{\theta}$ phase space, where $\bar{T}$ and $\bar{\theta}$ are the kinetic energy and angle of the outgoing pion in the center-of-mass system of the incident pion and the deuteron. Measurements were made with π^+ and π^- beams at incident kinetic energies of 256, 331, and 450 MeV. The momentum spread of the beams was $\Delta p/p=4\%$ and their intensities were approximately $2\times10^8\pi^-$/s and $10^9\pi^+$/s.

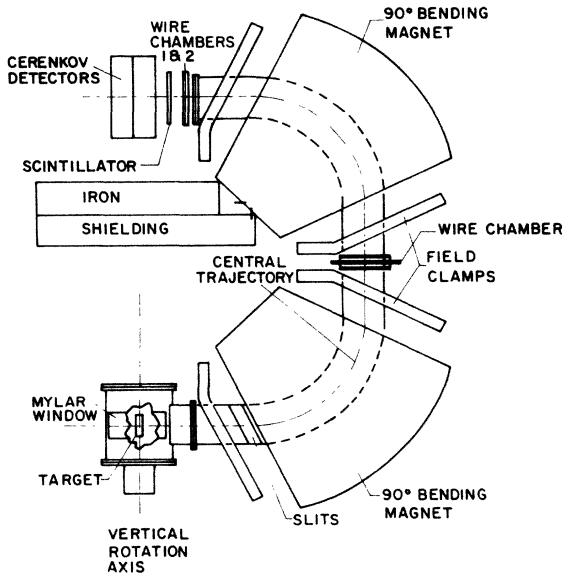

FIG. 1. A schematic description of the spectrometer.

The outgoing particles were detected by a 180° doubly focusing magnetic spectrometer[1,5–7] with a solid angle of 17 msr and momentum acceptance of $\pm4.8\%$. A schematic description of the spectrometer is shown in Fig. 1. The detection system consisted of a multiwire proportional chamber between the two dipole magnets of the spectrometer, a pair of multiwire proportional chambers immediately behind the focal plane, a 1.6-mm-thick plastic scintillation detector, a fluorocarbon (FC-88) threshold Čerenkov counter, and last, an Aerogel ($n=1.055$) Čerenkov counter. A quadruple coincidence among signals from the three wire-chamber delay lines and the scintillator defined an acceptable event. The last two wire chambers established the trajectory of a particle as it crossed the focal plane. For events that corresponded to allowed trajectories, pulse heights from the scintillator and Čerenkov detectors and the time of flight through the second bending magnet discriminated against electrons or, when set for positive charge, against positrons, protons, and other light nuclei. Corrections for pions decaying in the relatively short 3.5-m flight path and for muons that were recorded as good events were calculated with the Monte Carlo simulation DECAY TURTLE.[7] Additional details of the spectrometer and its detection system, as well as the particle identification procedure and the applied corrections, are given elsewhere.[1]

The target consisted of a cylindrical flask 2.5 cm in diameter mounted concentrically with the spectrometer's axis of rotation, that contained either liquid deuterium (99.83% deuterium) or liquid hydrogen. Background from the 50-μm Mylar target walls was measured with the flask empty. The incident pion flux was monitored with an ionization chamber as well as with a scattering monitor downstream from the spectrometer.

The measured pion-production cross sections were normalized to πp elastic scattering. At each incident energy, relative πp elastic cross sections were measured at several angles and the angular distribution was normalized to fit the "known cross sections" with a scale factor that calibrated the system as a whole. Below 300 MeV, the "known cross sections" were derived from the phase-shift analysis of Carter, Bugg, and Carter[8] using the routine SCATPI.[9] Above this energy they were interpolated directly from the measurements.[10] The interpolation procedure is described in Ref. 6 and is the same used to normalize the $\pi^-p\rightarrow\pi^+\pi^-n$ cross sections of Ref. 1.

III. RESULTS AND DISCUSSION

Figures 2–4 show the doubly differential cross sections for the $\pi^-d\rightarrow\pi^+\pi^-nn$ and $\pi^+d\rightarrow\pi^-\pi^+pp$ reactions at 256, 331, and 450 MeV. The errors shown in the figures represent the combination of statistical uncertainties and the systematic ones that depend on the outgoing pion momentum. The overall normalization is uncertain by an additional 4%. As can be seen from the figures, the π^-d and π^+d data agree within the experimental uncertainties.

Interpretation of these data is aided by comparison with two simple models of the reaction. The solid curves

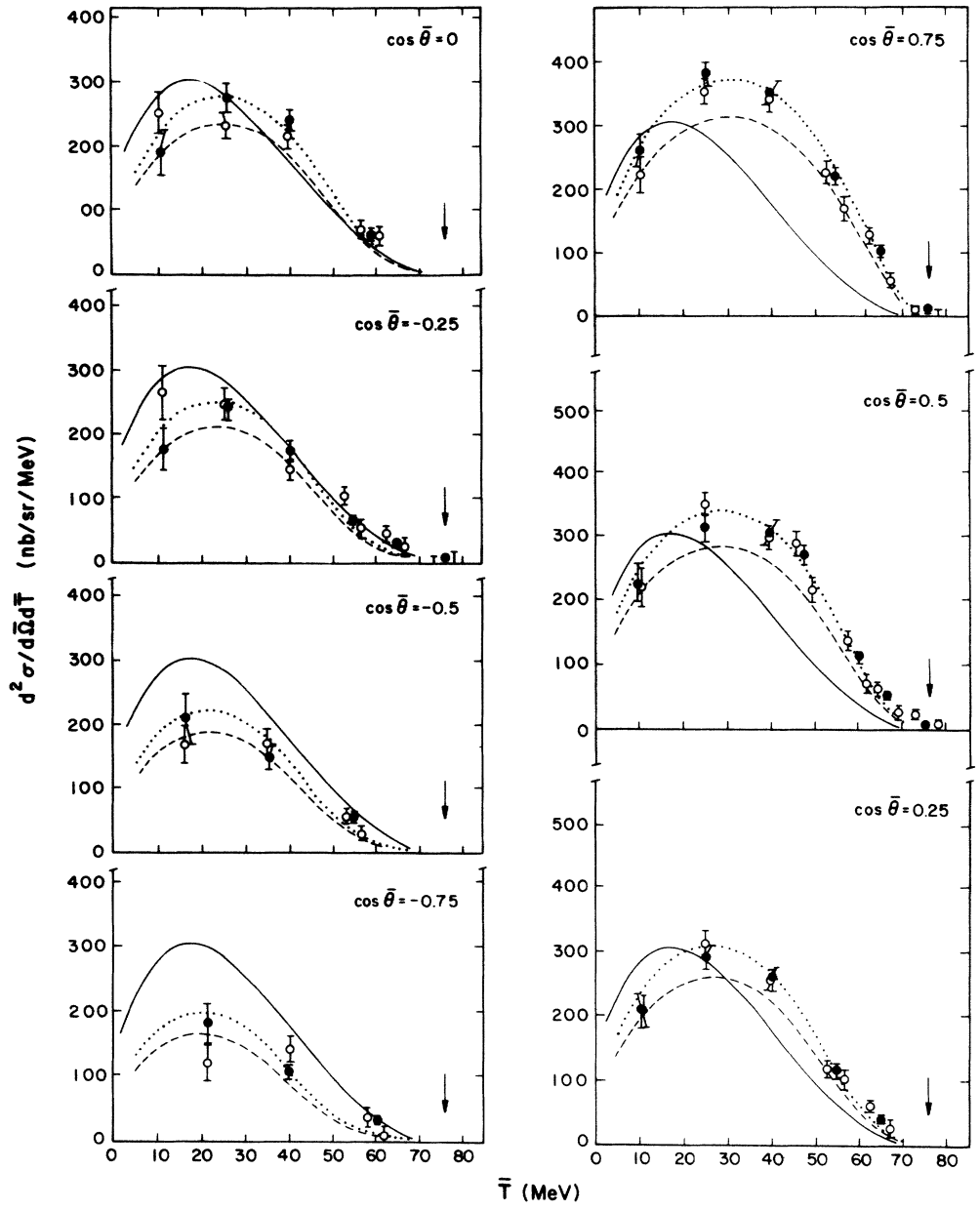

FIG. 2. Doubly differential cross sections for the $\pi^-d \rightarrow \pi^+\pi^-nn$ (solid circles) and for the $\pi^+d \rightarrow \pi^-\pi^+pp$ (open circles) reactions for $T_\pi^{in} = 256$ MeV. $\bar{T}$ and $\bar{\theta}$ are the outgoing π^+ (π^-) kinetic energy and angle in the center-of-mass systems of the incident pion and deuteron. The arrows mark the energy corresponding to the two-body $\pi(\pi NN)$ production with zero binding energy for the πNN system. The solid curves represent four-body phase space normalized to the data. The dashed and dotted lines are quasifree calculations in plane-wave approximation (see the text).

represent the distribution of events in the four-body phase space, normalized so that the distribution integrated over energy and angle will equal the integrated reaction cross section determined from the data.

The dashed curves are the predictions of a calculation based on plane-wave approximation of quasifree pion production on one nucleon with the use of a phenomenological on-shell amplitude deduced from the $\pi^-p \rightarrow \pi^+\pi^-n$ data.[1] Once this production amplitude is chosen, the quasifree calculation involves no other free parameters. A detailed description of the calculations is given in Sec. IV.

The quasifree calculations are in surprisingly good agreement with the general features of the data, although some discrepancies do exist. At 256 MeV the quasifree calculation reproduces the shape of the spectra very well, but the calculated total cross section is 20% below the measured result. The dotted curve in Fig. 2 is the quasifree calculation normalized by the ratio of the measured and the calculated integrated cross sections (i.e., by 1.25), which is in good agreement with the data. At 331 MeV both the shape and the integrated reaction cross section obtained from the quasifree calculation agree with the

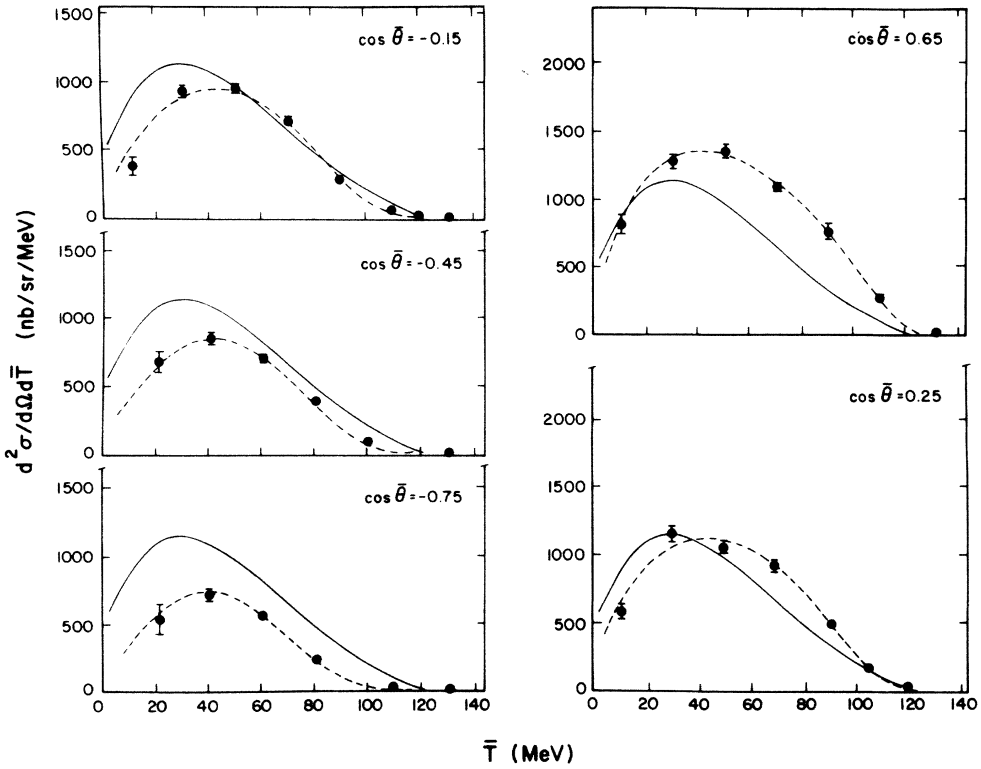

FIG. 3. Same as Fig. 2, for $T_\pi^{\text{in}} = 331$ MeV for the $\pi^- d \to \pi^+ \pi^- nn$ reaction only.

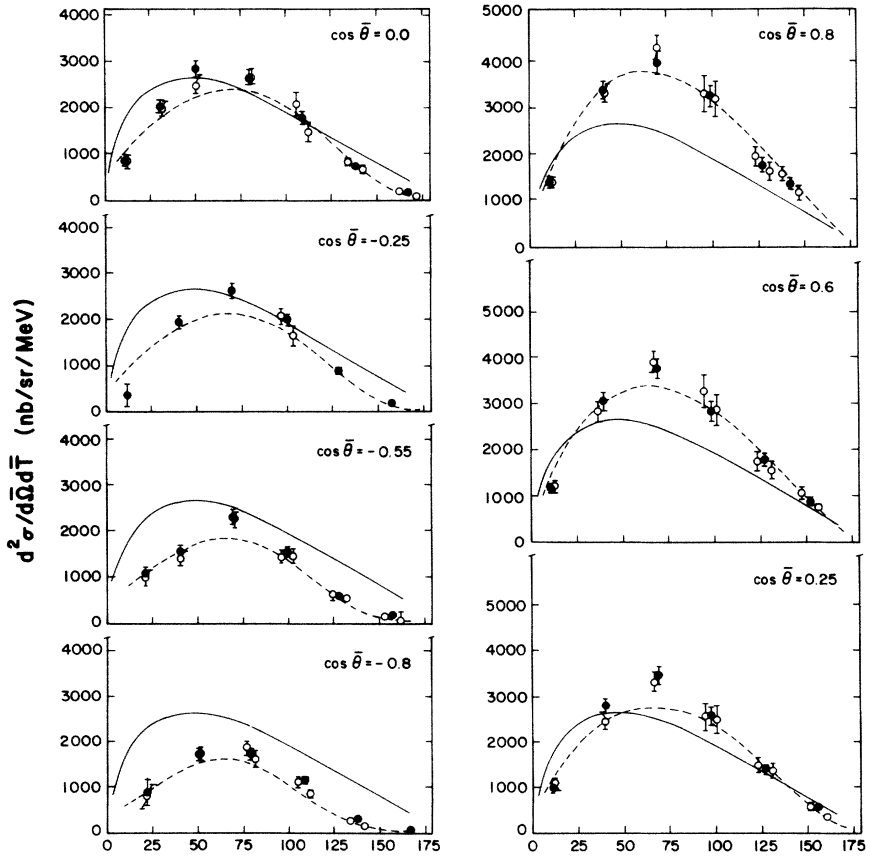

FIG. 4. Same as Fig. 2, for $T_\pi^{\text{in}} = 450$ MeV.

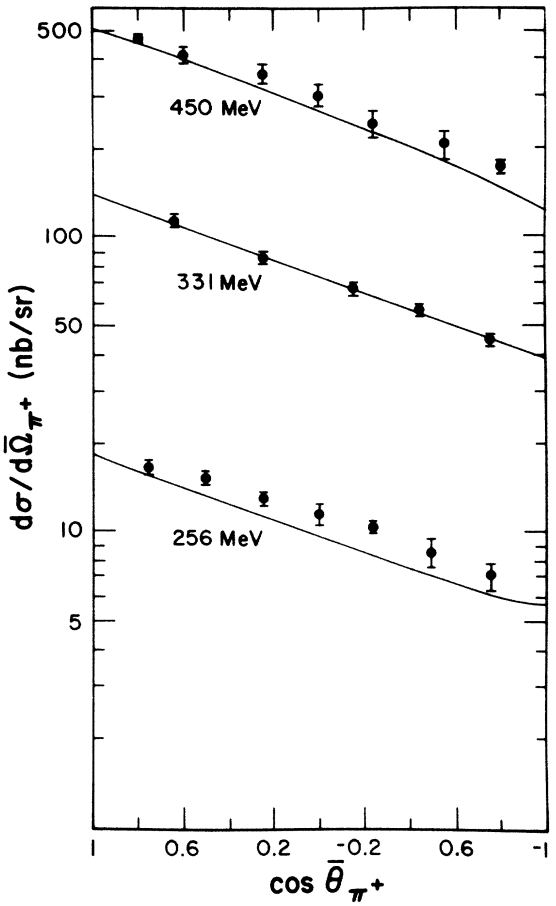

FIG. 5. The singly differential cross section for the $\pi^-d\to\pi^+\pi^-nn$ reaction at 256, 331, and 450 MeV. The lines are the quasifree calculations (see the text).

measurement within the experimental uncertainty. At 450 MeV there are some slight discrepancies between the calculated quasifree process and the data at backward angles.

The underestimation of the total cross section at 256 MeV may be due to rescattering processes of the pions or the final-state interaction of the two nucleons, which are not accounted for in the calculation. A more speculative explanation is the excitation of a three-body πNN resonance, which is discussed in Sec. V. The slight discrepancies between the data and the calculation at 450 MeV may indicate the incompleteness of the calculation, in which the elementary amplitude was parametrized only up to 550 MeV.

The measured doubly differential cross sections were integrated over the energy of the produced pion to determine singly differential cross sections and then over the angle to obtain the integrated reaction cross sections. To estimate the contribution from the unobserved kinematic range we assumed the form of the cross section given by the plane-wave approximation and assigned a 25% uncertainty to the contribution from the extrapolated region. The singly differential cross sections $d\sigma/d\bar{\Omega}_{\pi^+}$ are presented in Fig. 5 and the integrated reaction cross sections are given in Table I. We also present in Table I the measured integrated reaction cross sections for the free process $\pi^-p\to\pi^+\pi^-n$ and the prediction of the quasifree calculation. At this level of accuracy there is no discernible difference between the integrated reaction cross sections for pion-induced pion production on the deuteron and the proton. This, and the similarity between observation and the cross sections predicted by the simple quasifree calculation indicate that two-nucleon effects are probably not important in pion production on the deuteron. It will be interesting to compare this result with observation of the same reaction in heavier nuclei where two-nucleon effects should be more prevalent.

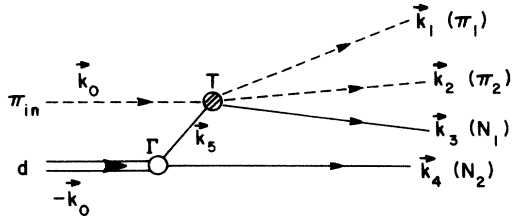

FIG. 6. Diagram of quasifree pion production on the deuteron.

IV. CALCULATIONS OF THE QUASIFREE PROCESS

In this section we derive the formulae used in the calculations of the quasifree single-nucleon pion production. The main goal is to establish the analytical relation between the $\pi d\to\pi\pi NN$ and the $\pi N\to\pi\pi N$ cross section [Eqs. (4.11) and (4.13)] so that the experimental cross section for pion-induced single-pion production on a nucleon can be used as input. Discrepancies between the data and calculated results will not only reflect those dynamical aspects not contained in the impulse approximation, but also pinpoint the kinematical regions that deserve future coincidence measurements.

The quasifree process in the plane-wave impulse approximation (PWIA) is illustrated in Fig. 6. Using the standard invariant normalization of plane-wave states,[11] we can express the spin-averaged total production cross section as

$$\sigma=\frac{1}{(2\pi)^8(2J+1)v_{\pi d}(\mathbf{k}_0)2w_{\mathbf{k}_0}2E_{d,\mathbf{k}_0}}$$
$$\times\sum_{m_J\nu'\mu'}\int\frac{d\mathbf{k}_4}{(E_{\mathbf{k}_4}/m_N)}\frac{d\mathbf{k}_3}{(E_{\mathbf{k}_3}/m_N)}\frac{d\mathbf{k}_2}{2w_{\mathbf{k}_2}}\frac{d\mathbf{k}_1}{2w_{\mathbf{k}_1}}\delta^{(3)}(\mathbf{k}_1+\mathbf{k}_2+\mathbf{k}_3+\mathbf{k}_4)\delta(w_{\mathbf{k}_1}+w_{\mathbf{k}_2}+E_{\mathbf{k}_3}+E_{\mathbf{k}_4}-W)$$
$$\times\left|\sum_{\mu}\langle\mathbf{k}_1,\mathbf{k}_2,\mathbf{k}_3\tfrac{1}{2}\mu'\,|\,A(W')\,|\,\mathbf{k}_0,\mathbf{k}_5\tfrac{1}{2}\mu\rangle\Phi_{\mu\nu',m_J}(\mathbf{Q})\right|^2, \tag{4.1}$$

TABLE I. Integrated reaction cross sections for the $\pi^-d\to\pi^+\pi^-nn$ and $\pi^-p\to\pi^+\pi^-n$ at 256, 331, and 450 MeV. The calculations are predictions of the quasifree model discussed in the text.

Incident energy (MeV)	$\pi^-p\to\pi^+\pi^-n$	$\pi^-d\to\pi^+\pi^-nn$	Quasifree calculation
256	166±6 μb[a]	160±10 μb	134 μb
331	1160±50 μb[a]	1000±100 μb	955 μb
450	4250±300 μb	3950±250 μb	3720 μb

[a]Results of Ref. 1.

where

$$v_{\pi d}(\mathbf{k}_0)=\frac{k_0 W}{w_{\mathbf{k}_0}E_{d,\mathbf{k}_0}} \tag{4.2}$$

is the relative velocity between the incoming pion and the deuteron in the c.m. system and

$$W\equiv w_{\mathbf{k}_0}+E_{d,\mathbf{k}_0}=(\mathbf{k}_0^2+m_\pi^2)^{1/2}+(\mathbf{k}_0^2+m_d^2)^{1/2}$$

represents the total energy of the πd system. In this work we use the relativistic energy so that $w_{\mathbf{k}_i}\equiv(\mathbf{k}_i^2+m_\pi^2)^{1/2}$, $(i=0,1,2)$, and $E_{\mathbf{k}_i}\equiv(\mathbf{k}_i^2+m_N^2)^{1/2}$, $(i=3,4)$. In Eq. (4.1) the factor $(2J+1)^{-1}$ is due to spin averaging. For the deuteron, $J=1$. The indices m_J, ν', and μ' denote the spin projections of the deuteron and the two final nucleons, respectively. (For conciseness in notation the isospin indices are not explicitly written but are understood.) Furthermore, $\mathbf{k}_5(\equiv-\mathbf{k}_0-\mathbf{k}_4)$ and μ are the momentum and spin projections of the off-mass-shell intermediate nucleon. $A(W')$ denotes the invariant $\pi N\to\pi\pi N$ amplitude at energy $W'=[(W-E_{\mathbf{k}_4})^2-\mathbf{k}_4^2]^{1/2}$; $\Phi(\mathbf{Q})$ is in principle a relativistic momentum-space deuteron wave function with $\mathbf{Q}\equiv\frac{1}{2}\mathbf{k}_0+\mathbf{k}_4$ being the internal momentum of the deuteron. Φ can be related to the s-d-state deuteron wave functions u and w by[12,13]

$$\Phi_{\mu\nu',m_J}(\mathbf{Q})=(2\pi)^{3/2}(2E_{d,\mathbf{k}_0}E_{\mathbf{k}_4}/E_{\mathbf{k}_5})^{1/2}$$
$$\times[u(Q)Y_{00}(\hat{Q})\langle\tfrac{1}{2}\mu\tfrac{1}{2}\nu'\mid lm_J\rangle-w(Q)\sum_{m_Lm_S}Y_{2m_L}(\hat{Q})\langle 2m_L,lm_S\mid lm_J\rangle\langle\tfrac{1}{2}\mu,\tfrac{1}{2}\nu'\mid lm_S\rangle], \tag{4.3}$$

where

$$E_{\mathbf{k}_5}\equiv[(\mathbf{k}_0+\mathbf{k}_4)^2+m_N^2]^{1/2}.$$

Using Eq. (4.3) and standard angular-momentum algebra, one can show that Eq. (4.1) is equivalent to

$$\sigma=\frac{m_d}{(2\pi)^5 3v_{\pi d}(\mathbf{k}_0)2w_{\mathbf{k}_0}}\int\frac{d\mathbf{k}_4}{E_{\mathbf{k}_5}/m_N}$$
$$\times\left[\int\frac{d\mathbf{k}_3}{E_{\mathbf{k}_3}/m_N}\frac{d\mathbf{k}_2}{2w_{\mathbf{k}_2}}\frac{d\mathbf{k}_1}{2w_{\mathbf{k}_1}}\delta^{(3)}(\mathbf{k}_1+\mathbf{k}_2+\mathbf{k}_3+\mathbf{k}_4)\delta(w_{\mathbf{k}_1}+w_{\mathbf{k}_2}+E_{\mathbf{k}_3}+E_{\mathbf{k}_4}-W)\right.$$
$$\left.\times\sum_{\mu'\mu}|\langle\mathbf{k}_1,\mathbf{k}_2,\mathbf{k}_3\tfrac{1}{2}\mu'\mid A(W')\mid\mathbf{k}_0,\mathbf{k}_5\tfrac{1}{2}\mu\rangle|^2\right]|R_\mu(Q)|^2 \tag{4.4}$$

with

$$|R_\mu(Q)|^2=\frac{3}{8\pi}[u(Q)]^2+9\begin{Bmatrix}2 & 1 & 1\\ 1/2 & 1/2 & 3/2\end{Bmatrix}^2[w(Q)]^2\sum_{m_L}|Y_{2m_L}(\hat{Q})|^2(\langle\tfrac{1}{2}\mu,2m_L\mid\tfrac{3}{2}\mu+m_L\rangle)^2. \tag{4.5}$$

The present theoretical results were obtained with the nonrelativistic deuteron wave functions given by the Reid soft-core potential.[14] The results of our calculations are not sensitive to a specific choice of the deuteron wave functions. Use of wave functions given by the Paris potential[15] or of the relativistic wave functions of Buck and Gross[12] has led to essentially identical results for pion energies studied in this work.

Let us denote the quantity inside the brackets of Eq. (4.4) by $S_{\mu',\mu}(W';m_1,m_2,m_3)$ with $m_1=m_2=m_\pi$ and $m_3=m_N$. In the center-of-mass frame of the subsystem (123) we have

$$S_{\mu'\mu}(W';m_\pi,m_\pi,m_N)\equiv\int\frac{d\mathbf{p}_3}{(E_{\mathbf{p}_3}/m_N)}\frac{d\mathbf{p}_2}{2w_{\mathbf{p}_2}}\frac{d\mathbf{p}_1}{2w_{\mathbf{p}_1}}\delta^{(3)}(\mathbf{p}_1+\mathbf{p}_2+\mathbf{p}_3)\delta(w_{\mathbf{p}_1}+w_{\mathbf{p}_2}+E_{\mathbf{p}_3}-W')$$
$$\times|\langle\mathbf{p}_1,\mathbf{p}_2,\mathbf{p}_3\tfrac{1}{2}\mu'\mid A(W')\mid\mathbf{p}_0,-\mathbf{p}_0\tfrac{1}{2}\mu\rangle|^2. \tag{4.6}$$

Here the momenta $\mathbf{p}_i$, $i=0,1,2,3$, are defined in the three-body c.m. frame. One can also write

$$S_{\mu'\mu}(W';m_\pi,m_\pi,m_N)=2m_N\left[\frac{\pi}{4}\right]\int dw_{\mathbf{p}_1}d\Omega_{\hat{\mathbf{p}}_1}\,|\langle\bar{A}_{\mu'\mu}(W',\mathbf{p}_1)\rangle|^2\frac{p_1X_1}{Z_1^2}\,, \tag{4.7}$$

with

$$Z_1^2=(W')^2-2w_{\mathbf{p}_1}W'+m_\pi^2 \tag{4.8}$$

and

$$X_1=\{[Z_1^2-(m_\pi-m_N)^2][Z_1^2-(m_\pi+m_N)^2]\}^{1/2}\,. \tag{4.9}$$

In Eq. (4.7) $|\langle\bar{A}_{\mu'\mu}(W',\mathbf{p}_1)\rangle|^2$ depends only on W' and $\mathbf{p}_1$, and thus represents the value of $|\langle A_{\mu'\mu}\rangle|^2$ averaged over all other kinematical variables. Using the relation

$$\sigma_{\pi N\to\pi\pi N}(W';\mu',\mu)=\frac{m_N}{(2\pi)^5v_{\pi N}(\mathbf{p}_0)2w_{\mathbf{p}_0}E_{\mathbf{p}_0}}\times S_{\mu'\mu}(W';m_\pi,m_\pi,m_N)\,, \tag{4.10}$$

with $v_{\pi N}(\mathbf{p}_0)=p_0W'/(w_{\mathbf{p}_0}E_{\mathbf{p}_0})$, we obtain for Eq. (4.4)

$$\sigma=\tfrac{1}{3}\int d\mathbf{k}_4\left[\frac{p_0W'm_d}{k_0WE_{\mathbf{k}_4+\mathbf{k}_0}}\right]\sum_{\mu'\mu}\sigma_{\pi N\to\pi\pi N}(W';\mu',\mu)\times|R_\mu(Q)|^2\,. \tag{4.11}$$

This last equation enables the calculation of $\sigma(\pi d\to\pi\pi NN)$ with experimental $\sigma(\pi N\to\pi\pi N)$ as input.

Since the existing experimental $\sigma(\pi N\to\pi\pi N)$ are spin-averaged cross sections, it is useful to introduce into Eq. (4.4) a spin-averaging approximation defined by

$$\sum_{\mu'\mu}\sigma_{\pi N\to\pi\pi N}(W';\mu',\mu)\,|R_\mu(Q)|^2\simeq|R(Q)|^2\sum_{\mu'\mu}\sigma_{\pi N\to\pi\pi N}(W';\mu',\mu)\,, \tag{4.12}$$

with

$$|R(Q)|^2\equiv\tfrac{1}{2}\sum_{\mu''}|R_{\mu''}(Q)|^2\,.$$

Introducing Eqs. (4.12), (4.10), and (4.7) into (4.11) and defining

$$|\langle\bar{A}(W',\mathbf{p}_1)\rangle|^2=\tfrac{1}{2}\sum_{\mu'\mu}|\langle\bar{A}_{\mu'\mu}(W',\mathbf{p}_1)\rangle|^2\equiv p_0^2\langle\bar{M}^2\rangle\,,$$

we obtain

$$\frac{d^2\sigma}{dw_{\mathbf{k}_1}d\cos\theta_{k_1}}=\frac{d^2\sigma}{dT_1d\cos\theta_{k_1}}=\frac{m_N^2E_{d,\mathbf{k}_0}}{96\pi^3k_0W}\int\frac{d\mathbf{k}_4}{E(\mathbf{k}_4+\mathbf{k}_0)}\frac{k_1X_1}{Z_1^2}p_0^2\overline{\langle M(W',\mathbf{p}_1)^2\rangle}\,|R(Q)|^2\,. \tag{4.13}$$

Here T_1 and θ_{k_1} (denoted henceforth $\bar{T}$ and $\bar{\theta}$, respectively) are the kinetic energy and polar angle of the detected pion [π^+ in $\pi^-d\to\pi^+(\pi^-nn)$ and π^- in $\pi^+d\to\pi^-(\pi^+pp)$ reactions] in the πd c.m. frame. In obtaining Eq. (4.13), we have also used the relation

$$p_1dw_{\mathbf{p}_1}d\Omega_{\hat{\mathbf{p}}_1}=d\mathbf{p}_1/w_{\mathbf{p}_1}=d\mathbf{k}_1/w_{\mathbf{k}_1}\,.$$

We have parametrized the quantity $\langle\bar{M}^2\rangle$ along the lines of Ref. 6. We used the following parametrization.

$$\overline{\langle M(\sqrt{s},\mathbf{q})^2\rangle}=(A_1+A_4\bar{q}^4)+\left[A_2+\frac{A_5}{A_6+\bar{q}^4}\right]\times\bar{q}\cos\theta^*+A_3(\bar{q}\cos\theta^*)^2 \tag{4.14}$$

with

$$\bar{q}=q/q_{\max}\,, \tag{4.15}$$

$$q_{\max}=\sqrt{(m_\pi+T_{\max})^2-m_\pi^2}\,, \tag{4.16}$$

$$T_{\max}=\frac{1}{2\sqrt{s}}[(\sqrt{s}-m_\pi)^2-(m_\pi+m_N)^2]\,, \tag{4.17}$$

and

$$\sqrt{s}=\sqrt{(m_\pi+m_N)^2+2m_NT_{\pi,\mathrm{lab}}}\,. \tag{4.18}$$

Here $T_{\max}$ is the maximum pion kinetic energy in the c.m. frame of the $\pi\pi N$ three-body system with a total c.m. energy $\sqrt{s}$. The q and θ^* are the c.m. momentum and angle of the measured pion. Since $\bar{q}$ is dimensionless, the coefficients A_i ($i=1$ to 6) carry the same units as $\langle\bar{M}^2\rangle$, which is (energy^{-6}). The coefficients for the different measured energies[6] are presented in Table II. Their energy dependence is represented by a polynomial in $T_{\pi,\mathrm{lab}}$. We have determined the A_i's from fitting a large body of experimental doubly differential cross sections $d^2\sigma_{\pi^+}/dT_{\pi^+}d\cos\theta_{\pi^+}$ for the reaction $\pi^-p\to\pi^+\pi^-n$ at pion laboratory kinetic energies 210–550 MeV. When the $\langle\bar{M}^2\rangle$ is used for calculating single-pion production in the deuteron via Eq. (4.23), the variables $\sqrt{s}$ and $\mathbf{q}$ of Eq. (4.24) are replaced by the corresponding variables W' and $\mathbf{p}_1$ of the four-body system.

The theoretical results are shown along with the experimental data in Figs. 2–4. The overall agreement between the calculations and the data is good. Some existing deviations were discussed in Sec. III.

TABLE II. The parameters, A_i, obtained by fitting the $\pi^-p\to\pi^+\pi^-n$ data to the expression Eq. (4.14). The data at each energy are from the reference in the last column.

T_π (MeV)	A_1 (m_π^{-6})	A_2 (m_π^{-6})	A_3 (m_π^{-6})	A_4 (m_π^{-6})	A_5 (m_π^{-6})	A_6	χ^2/ν	Reference
203	16.5	6.9					0.57	6
230	19.9	7.9					0.63	6
256	25.0	8.3					0.95	6
280	33.6	8.1					1.52	6
292	45.8	0.1		−22.8			0.53	6
331	54.2	−8.9	−7.5	−24.6	4.5	0.0400	1.31	6
358	64.5	−10.6	−11.8	−37.7	4.7	0.0130	0.80	6
450	67.2	−30.5	−24.3	−59.2	10.2	0.0465	1.87	16
516	35.1	−28.6	5.0	−26.9	19.3	0.2160	2.65	17
550	27.8	−42.8	11.9	−15.2	23.7	0.1530	2.00	17

V. BOUND πNN SYSTEMS

The possibility that a bound-state πNN system may exist was first investigated by Gale and Duck[18] within the framework of the nonrelativistic Faddeev equations, using a model of a rank-one separable potential for the pion-nucleon interaction in the P_{33} channel without including any nucleon-nucleon interaction. Their study did not support the existence of πNN bound states, not even when they included relativistic kinematics in the Faddeev equations. In subsequent works by Ueda[19] and by Kalbermann and Eisenberg,[20] this system was investigated using the Heitler-London-Pauli variational method in a nonrelativistic approach. These works, like the previous one, did not predict such bound states. However, the possible existence of a quasibound system was not ruled out by these authors. Recently the first calculation based on relativistic Faddeev equations, including both pion-nucleon and nucleon-nucleon interactions, was done by Garcilazo.[3] He used newly constructed pion-nucleon separable potentials that reproduce the phase shift of the P_{33} channel up to 350 MeV, and different realistic nucleon-nucleon interactions such as the Reid soft-core, Paris, and Malfliet-Tjon potentials. He found that bound-state solutions are possible when a sufficiently short ranged pion-nucleon interaction is assumed. Observation of such states and the measurement of the cross sections (or even upper limits on the cross sections) for its formation is therefore interesting.

A resonance in the π^-nn (π^+pp) system would appear as an enhancement of the production cross section for $\pi^-d\to\pi^+(\pi^-nn)$ [$\pi^+d\to\pi^-(\pi^+pp)$]. A bound state would appear as a peak at an energy beyond the upper edge of the phase allowed for production. In Fig. 2 the arrows mark the energy corresponding to two-body $\pi(\pi NN)$ production with zero binding energy for the πNN system. The low cross sections measured at the high-energy edge of the four-body phase space show no evidence for the production of a weakly bound πNN system. We can set upper limits on the cross section for the formation of bound π^-nn and π^+pp systems in the two reactions, and the results are presented in Table III.

For a given setup of the spectrometer (central momentum, energy—P_{cent},E_{cent}) we measure the number of particles detected in all or part of the focal plane to obtain $\Delta\sigma/\Delta\Omega\Delta E\ \pm\delta$, where $\Delta\Omega$ is the solid angle and ΔE the energy acceptance; δ is the total uncertainty, including statistical and systematic uncertainties. The upper limit for a bound-state excitation with binding energy ϵ_B (given in Table III) is defined as follows:

$$\left.\frac{d\sigma}{d\Omega}\right|_{\substack{\text{upper}\\ \text{limit}}} = \frac{(\Delta\sigma/\Delta\Omega\Delta E + 2\delta)}{\frac{1}{\sqrt{2\pi}}\int e^{-1/2(E-E_B)^2/\sigma^2}\cdot \text{ACCP}(E-E_{\text{center}})dE},$$

TABLE III. Upper limits for formation of bound π^-nn and π^+pp systems in the $d(\pi^-,\pi^+)\pi^-$nn and $d(\pi^+,\pi^-)\pi^+$pp reactions. (Over narrower angular ranges these upper limits are two to three times smaller.)

T_π (MeV)	Reaction (system)	Binding energy range (MeV)	Angular range ($\bar{\theta}$) (deg)	Upper limit (nb/sr)
256	$d(\pi^+,\pi^-)$ (π^+pp)	0–6	40–105	200
256	$d(\pi^-,\pi^+)$ (π^-nn)	0–6	40–105	300
331	$d(\pi^-,\pi^+)$ (π^-nn)	0–10	50–140	500
331	$d(\pi^-,\pi^+)$ (π^-nn)	0–20	99–101	500

where E_B is the laboratory energy corresponding to a system with binding energy ϵ_B, σ is the standard deviation of the energy resolution determined from the elastic-scattering measurements, and ACCP $(E-E_{\text{center}})$ is the spectrometer acceptance function normalized so that

$$\int \text{ACCP}(E-E_{\text{center}})dE=1 .$$

The integration is over the part of the focal plane used to obtain $\Delta\sigma/\Delta\Omega\Delta E$. These upper limits were determined predominantly by the statistics of the measurements and the energy resolution of the system. The energy resolution, determined mainly by the beam, was about 12, 10, and 8.5 MeV for the 331-MeV π^-, 256-MeV π^-, and 256-MeV π^+ measurements, respectively.

The deviation between the data and the quasifree calculation at 256 MeV is rather puzzling in light of the good agreement with the calculation at the higher energies. Even though no structure indicating a bound πNN state is observed experimentally, some features in the 256-MeV results may lead one to speculate on the existence of a resonance in the three-body system. Indeed, such a resonance will show itself as a deviation from the four-body phase space and may have some angular dependence. To test this idea we made the artificial assumption that the

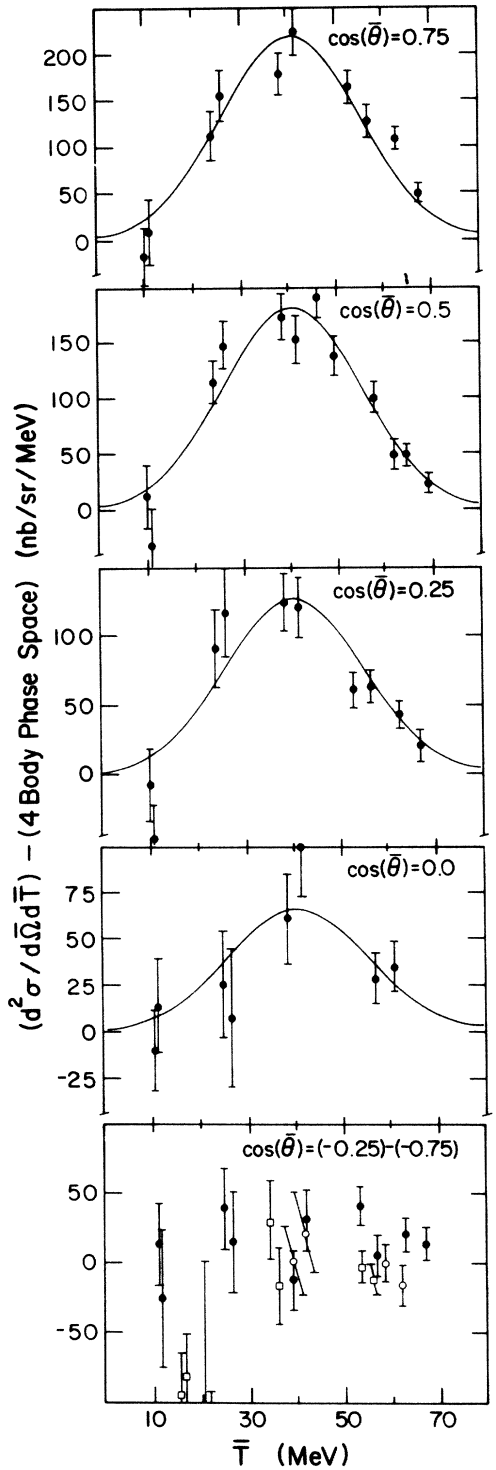

FIG. 7. The difference between the measured doubly differential cross section and the four-body phase space normalized to the data at backward angles. The solid lines are Gaussians fitted to the data. Amplitude, width, and position are fitted parameters. The incident pion energy is 256 MeV and the data are from the reaction $\pi^-\text{d}\rightarrow\pi^+\pi^-\text{nn}$.

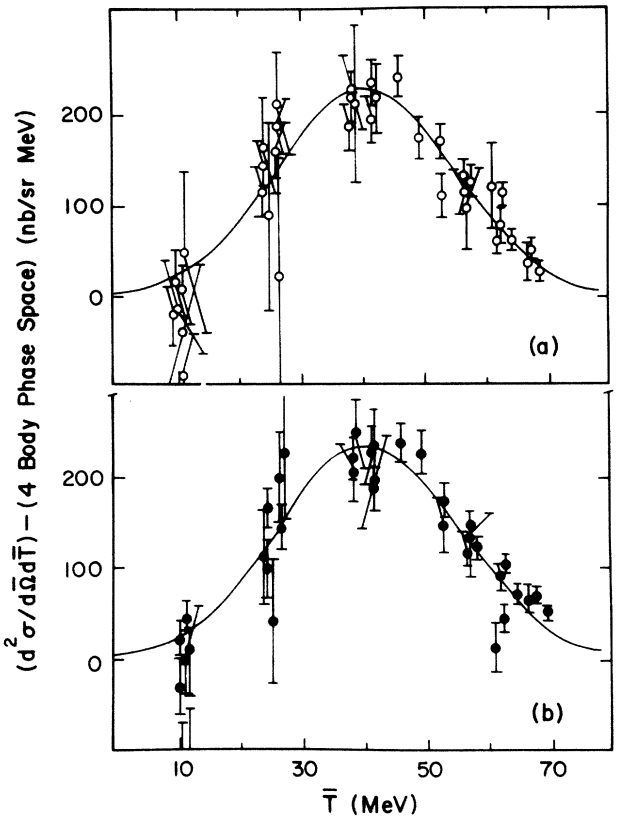

FIG. 8. The difference between the measured doubly differential cross section and four-body phase space normalized to the data. All the data measured at $T_\pi^{\text{in}}=256$ MeV and $\cos\bar{\theta}=0.75$, 0.5, 0.25, 0.0 are presented for $\pi^-\text{d}\rightarrow\pi^+\pi^-\text{nn}$ in (a) and for $\pi^+\text{d}\rightarrow\pi^-\pi^+\text{pp}$ in (b). The data corresponding to different $\cos\bar{\theta}$ and are normalized by the ratio of amplitude of the fitted Gaussians presented in Fig. 7.

cross section at 256 MeV was the incoherent sum of a term proportional to the phase space plus a "residual" cross section. To estimate the first contribution, the four-body phase-space distribution was normalized to the data at backward angles. This normalized phase-space distribution, which has the same shape at all angles, was subtracted from data at three forward angles. The "residual" cross section at each angle was fitted with a Gaussian that proved to have a centroid at 42 ± 2 MeV and a width of 33.5 ± 1.5 MeV (Figs. 7 and 8) at all the measured forward angles. Integrating the extracted Gaussians over energy, one obtains the angular behavior of the "residual" cross section. From this one can roughly estimate the total residual cross section to be about 25% of the total $\pi^{\pm}d\rightarrow\pi^{\mp}\pi^{\pm}NN$ cross section at 256 MeV. The same procedure applied to the 331- or 450-MeV data did not yield residual cross sections with constant centroids or widths. This result is consistent with the idea that such a resonance, if existing, would be more readily excited at the lower energy due to the lower momentum transfer.

In summary, although these results are not inconsistent with speculations about πNN resonances, it is evident that quasifree production on single nucleons is the dominant process and that there might be other reasons for the discrepancy.

VI. SUMMARY

We have presented the results of measurements of pion-induced pion production on the deuteron and compared them to pion production on the proton. The total cross sections for $\pi^-d\rightarrow\pi^+\pi^-nn$ and $\pi^-p\rightarrow\pi^+\pi^-n$ are found to be equal at 256, 331, and 450 MeV. The doubly differential cross sections for $\pi^+d\rightarrow\pi^-\pi^+pp$ and $\pi^-d\rightarrow\pi^-\pi^+nn$ are also found to be nearly equal.

A calculation of the quasifree process, using on-shell experimental amplitudes, was performed in plane-wave approximation. It agrees very well with the shape of the measured doubly differential cross section throughout the observed angular and energy range. Its normalization is 20% below the 256-MeV experimental results, but agrees at both 331 and 450 MeV. At all energies the shape of the four-body phase space resembles the data at backward angles, but falls below the high-energy part of the cross section at forward angles. The dominant process seen in the these data appears to be the quasifree production on a single nucleon.

Our results show no evidence for two-nucleon production mechanisms, as could have been *a priori* anticipated for the two-body system. Further pion production experiments should be carried out on heavier systems where contributions due to two-nucleon mechanisms—such as $\Delta N\rightarrow\Delta\Delta$—would be significantly enhanced. The observed discrepancy between our data and the quasifree calculations presented in this paper, even if relatively small, call for detailed microscopic theories which account for both the reaction mechanism and final state interaction.

ACKNOWLEDGMENTS

We would like to thank J. L. Matthews, E. R. Kinney, and S. Hoibraten for their help throughout the experiment. We would also like to thank the LAMPF staff for their assistance and support. Illuminating discussions with G. E. Brown, J. M. Eisenberg, H. Garcilazo, F. Lenz, H. Toki, and A. Wirzba are gratefully acknowledged. This work was supported in part by the U.S. Department of Energy and the Israeli Commission for Basic Research.

---

*Present address: MIT, Cambridge, MA 02139.
†Present address: Tel Aviv University, Tel Aviv, Israel.

[1]C. W. Bjork *et al.*, Phys. Rev. Lett. **44**, 62 (1980). A bibliography of previous works is given in this reference.
[2]G. E. Brown, H. Toki, W. Weise, and A. Wirzba, Phys. Lett. **118B**, 39 (1982).
[3]H. Garcilazo, Phys. Rev. C **26**, 2685 (1982); Phys. Rev. Lett. **50**, 1567 (1983); Nucl. Phys. **A408**, 559 (1983).
[4]E. Piasetzky *et al.*, Phys. Rev. Lett. **53**, 540 (1984).
[5]A. T. Oyer, Los Alamos National Laboratory Report LA-6599-T, 1976; J. B. Walter, Los Alamos National Laboratory Report LA-8377-T, 1979.
[6]D. Manley, Los Alamos National Laboratory Report LA-9101-T, 1981.
[7]S. A. Wood, Los Alamos National Laboratory Report LA-9932-T, 1983.
[8]J. R. Carter, D. V. Bugg, and A. A. Carter, Nucl. Phys. **B58**, 378 (1973).
[9]J. B. Walter and G. A. Rebka, Jr., Los Alamos National Laboratory Report LA-7731-MS, 1979.
[10]P. J. Bussey *et al.*, Nucl. Phys. **B59**, 363 (1973); H. R. Rugge and O. T. Vik, Phys. Rev. **129**, 2300 (1963); and P. M. Ogden *et al.*, *ibid.* **137**, B1115 (1965).
[11]J. D. Bjorken and S. D. Drell, in *Relativistic Quantum Mechanics* (McGraw-Hill, New York, 1964), p. 285.
[12]F. Gross, Phys. Rev. D **10**, 223 (1974); and W. W. Buck and F. Gross, *ibid.* **20**, 2361 (1979). Our Eq. (4.4) corresponds to the χ^+ solution of F. Gross.
[13]The spinors are treated nonrelativistically.
[14]R. Reid, Ann. Phys. (N.Y.) **50**, 411 (1968).
[15]M. Lacombe *et al.*, Phys. Rev. C **21**, 861 (1980); Phys. Lett. **101B**, 139 (1981).
[16]E. Piasetzky *et al.* (unpublished).
[17]D. C. Giancoli *et al.*, Phys. Rev. **154**, 1250 (1967).
[18]W. A. Gale and I. M. Duck, Nucl. Phys. **B8**, 109 (1968).
[19]T. Ueda, Phys. Lett. **74B**, 123 (1978).
[20]G. Kalbermann and J. M. Eisenberg, J. Phys. G **5**, 35 (1977).